PROCEEDINGS OF SCIENCE

Study of fragmentation reactions of light nuclei

D.A. Toneli[*a†], **B.V. Carlson**[a], **R. Donangelo**[b,c] **and S.R. Souza**[b,d]

[a] *Departamento de Física, Instituto Tecnológico de Aeronáutica*
CTA, 12.228-900, São José dos Campos, Brazil
[b] *Instituto de Física, Universidade Federal do Rio de Janeiro*
Cidade Universitária, CP 68.528, 21.941-972, Rio de Janeiro, Brazil
[c] *Instituto de Física, Facultad de Ingeniería, Universidad de la República*
Julio Herrera y Reissig, 565, 11.300, Montevideo, Uruguay
[d] *Instituto de Física, Universidade Federal do Rio Grande do Sul*
Av. Bento Gonçalves, 9.500, CP 15.051, 91.501-970, Porto Alegre, Brazil

The decay of the compound nucleus is traditionally calculated using a sequential emission model, such as the Weisskopf-Ewing or Hauser-Feshbach ones, in which the compound nucleus decays through a series of residual nuclei by emitting one particle at a time until there is no longer sufficient energy for further emission. In the case of light compound nucleus, however, the excitation energy necessary to fully disintegrate the system is relatively easy to attain. In such cases, decay by simultaneuous emission of two or more particles becomes important. A model which takes into account these decays is the Fermi break-up model. Recently, the Fermi break-up model was shown to be equivalent to the statistical multifragmentation model used to describe the decay of highly excited fragments from heavy ion reactions when the residual nuclei have few excited states. Due the simplicity of the thermodynamic treatment used in the multifragmentation model, we have adapted it to the calculation of Fermi breakup of light nuclei in a general context. The ultimate goal of this study is to calculate the distribution of isotopes produced in proton-induced reactions on light nuclei of biological interest, such as C, O and Ca. Although most of their residual nuclei possess extremely short half-lives and thus represent little long-term danger, they tend to be neutron-deficient and to decay by positron emission, which allows the monitoring of proton radiotherapy by PET ('positron emission tomography').

XXXIV edition of the Brazilian Workshop on Nuclear Physics

[*] Speaker.
[†] DAT is supported by CAPES. BVC acknowledges by support from FAPESP and the CNPq.

PoS(XXXIV BWNP)143

1. Introduction

The fragmentation of a highly-excited compound nucleus may be described by the Fermi break-up [1] or the statistical multifragmentation model [2-5]. The Fermi break-up model has traditionally been used for light nuclei (A$\leq$16). In both models, the result of a collision between two nuclei is assumed to be a highly excited, equilibrated system in a small volume of space. According to Fermi's golden rule, the transition rate for formation of an arbitrary fragment partition is proportional to the squared transition matrix element times the density of final states. Assuming that all transition matrix elements are identical, the transition rate for the formation of an arbitrary configuration of fragments can be estimated in terms of its density of states, obtained by integrating over its phase space with the restrictions of total energy and momentum conservation:

$$\omega_n = \prod_{l=1}^{n} \frac{1}{N_l!} \frac{1}{m_0^{3/2}} \prod_{j=1}^{n} g_j m_j^{3/2} \left[\frac{V_n}{(2\pi)^{3/2}\hbar^3} \right]^{n-1} \frac{E_{kin}^{\frac{3(n-1)}{2}-1}}{\Gamma\left[\frac{3(n-1)}{2}\right]}, \tag{1.1}$$

where the permutation factor $\prod_{l=1}^{n} 1/N_l!$ takes into account the indistinguishability of fragments with the same Z and A, m_j is the mass of each of fragment, $m_0 = \sum_{j=1}^{n} m_j$ is the mass of the decaying nucleus, g_j is the spin multiplicity of the fragment and V_n is the volume of the fragmenting nucleus, defined as:

$$V_n = (1+\chi)V_0, \tag{1.2}$$

where χ is the expansion factor and V_0 is the ground state volume of the nucleus. The total kinetic energy of the fragments, E_{kin} is given by:

$$E_{kin} = \varepsilon_0 - B_0 - E_{c0} + \sum_{j=1}^{n} (B_j + E_{cj}), \tag{1.3}$$

where the total excitation energy is ε_0, the ground state binding energy and the Coulomb energy of the decaying nucleus are B_0 and E_{c0}, respectively, while those of fragment j are denoted by B_j and E_{cj}.

The Fermi break-up model, as normally used [5], extends the expression above by taking into account all states of the fragments below the particle-emission threshold. In both of these cases, as well as that of a continous density of states, the density of final states can be well approximated in terms of the entropy S_n, the specific heat $C_{V,n}$ and the temperature T_0 [6] as:

$$\omega_n = \frac{e^{S_n(T_0)}}{\sqrt{2\pi C_{V,n} T_0^2}}, \tag{1.4}$$

This expression is very similar to that used in the microcanonical treatment of the statistical multifragmentation model:

$$\omega_n = e^{S_n(T_0)}. \tag{1.5}$$

In both cases, S_n is the entropy corresponding to a specific breakup channel parametrized by set of fragment multiplicities$\{N_{A,Z}\}$. The denominator of Eq. 1.4 arises from the steepest descent approximation to the integral defining the total density of states [6] but is usually neglected in the statistical multifragmentation model.

2. SMM and Fermi3 codes

The SMM code [7] uses the statistical multifragmentation model to calculate the fragmentation process of a highly-excited compound nucleus. The Fermi3 code we have developed is based on the Fermi break-up model. It permits calculation of the emission of fragments in the ground state alone (FB-GS), the emission of fragments restricted to the particle-bound excited levels (FB-PB) or the emission of fragments including all known excited levels plus the continuous density of states of the SMM (FB-CD). Both codes have been adapted to use the Audi-Wapstra mass table and to reproduce the Gilbert-Cameron level density parameter at low excitation energies which can be found at [8]. The entropy and the temperature are calculated by requiring energy conservation and both codes furnish the same value of the entropy in the case of a continuous density of excited states. The difference between the models is the Monte Carlo method used by the SMM code to select partitions versus the consideration of all partitions by the Fermi3 code, as well as the slowly varying factor in the denominator of the Fermi3 density of final states.

3. Fragmentation of ^{16}O

The figures below show the primary fragment charge and mass distributions resulting from the fragmentation of ^{16}O at an excitation energy of 5 MeV/nucleon for four different calculations. The calculations were performed using the SMM code. The other calculations used the Fermi3 code, in which only fragment ground states were included in the FB-GS calculation, all particle-bound excited states were included in the FB-PB calculation and the same continuous density of states of the SMM calculation was used in the case of the FB-CD calculation.

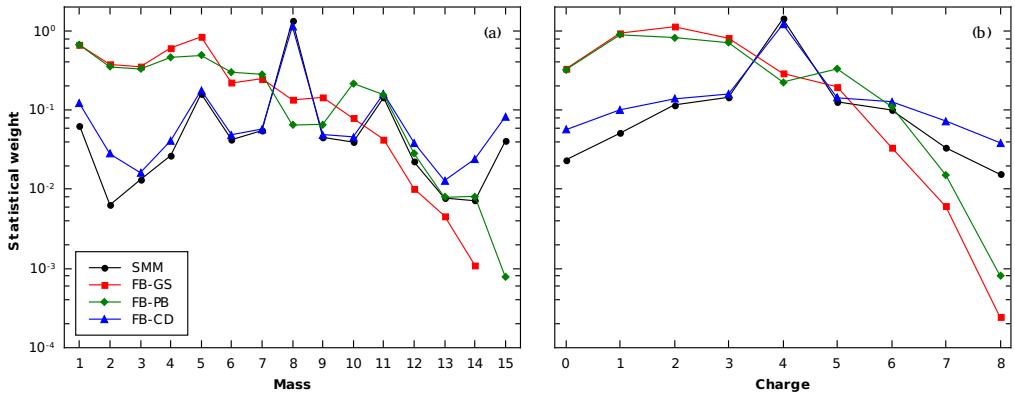

Figure 1: Primary mass (a) and charge (b) distribution of the multifragmentation of ^{16}O at an excitation energy of 5 MeV/nucleon.

Note that the results for the Fermi break-up model with continuum energy spectra are close to the results obtained with the statistical multifragmentation model but very different from those including only the ground or particle-bound excited states. Slight differences in the SMM and Fermi3 results are due to the differences in partition sampling and the factor in the denominator of the Fermi3 density of states.

In the Figure 2, we show the primary distributions of Li, Be, B and C isotopes resulting from the fragmentation of the same nucleus ^{16}O at the same excitation energy of 80 MeV. We again note the similarity of the results of the continuum Fermi break-up and statistical multifragmentation models, which are quite different from those including only the ground or particle-bound excited states.

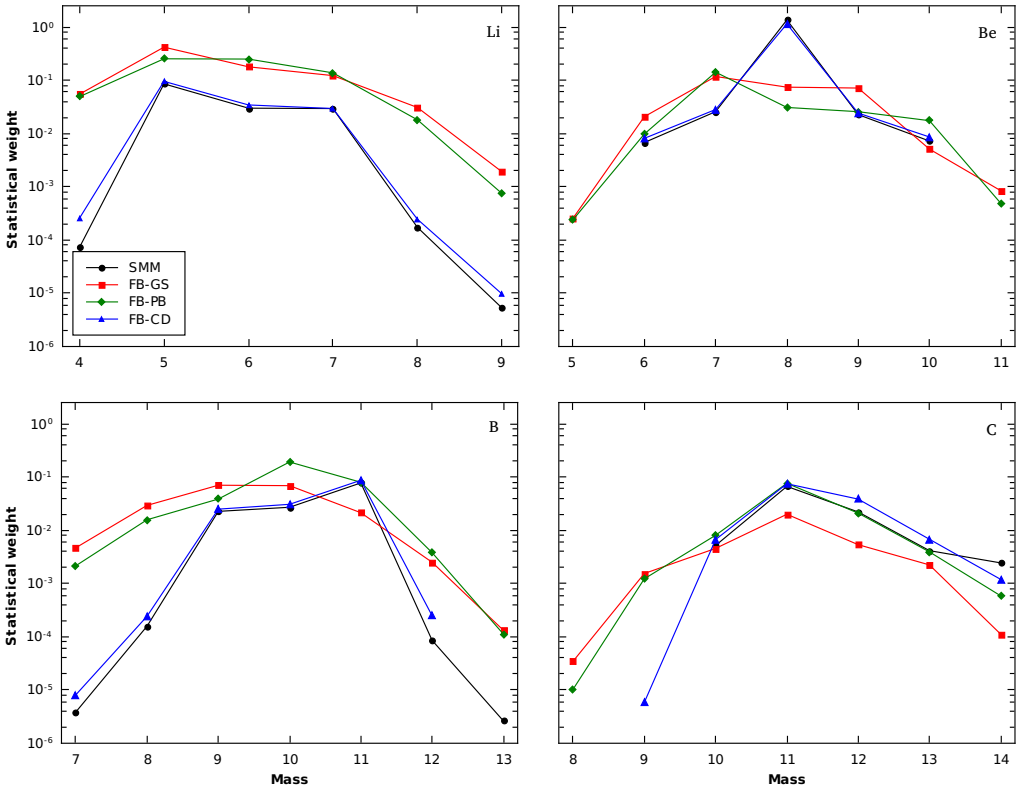

Figure 2: Primary isotopic distributions from the multifragmentation of ^{16}O at an excitation energy of 5 MeV/nucleon.

The Fermi3 code provides the average temperature and energy of fragments, as well as the probability and number of configurations of each multiplicity, information that we plan to use to estimate secondary decay of the fragments.

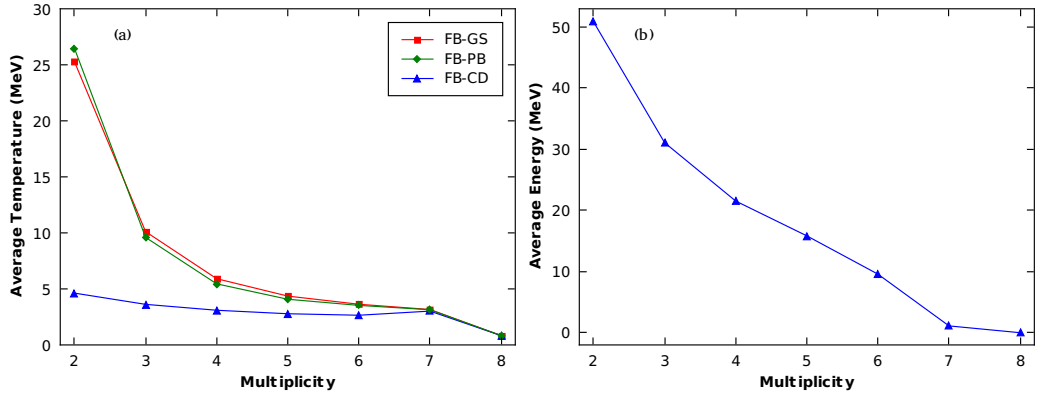

Figure 3: Average temperature (a) and excitation energy (b) of the fragments from the multifragmentation of ^{16}O at an excitation energy of 5 MeV/nucleon as a function of the multiplicity.

Note the extremely high temperatures at low multiplicity in the case of Fermi breakup including only ground or particle-bound states (FB-GS and FB-PB). This is due to the fact that none (FB-GS) or very little (FB-PB) of the excitation energy can be deposited in the fragments and thus, in these cases, it must be released as the kinetic energy in these cases. The average temperature varies much more slowly when the kinetic energy is in equilibrium with the fragment excitation energy (FB-CD). However, even here the average fragment excitation energy decreases rapidly with the increase of the multiplicity.

About 500 fragmentation partitions are available to the ^{16}O nucleus at an excitation energy of 80 MeV (5 MeV/nucleon). The greatest number of these correspond to multiplicities 4 and 5, with the distribution in multiplicity fairly symmetric about the maximum.

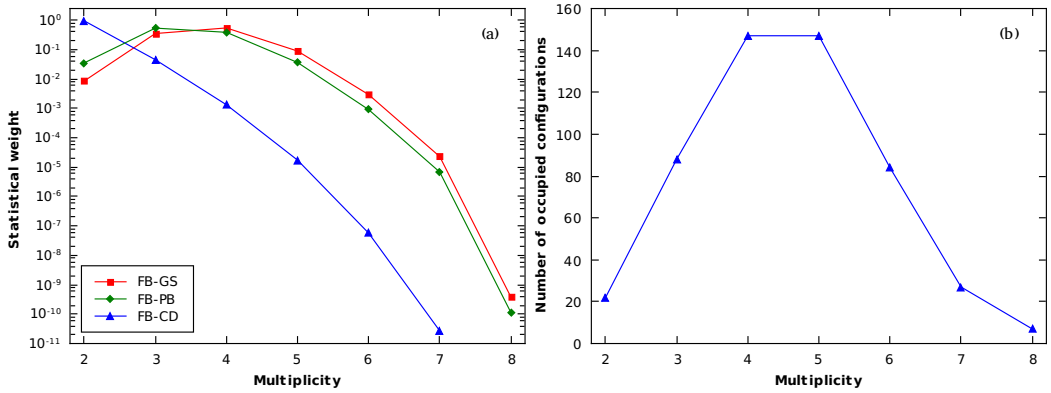

Figure 4: Average occupation statistical weight (a) and number of fragmentation partitions (b) as a function of the multiplicity for the multifragmentation of ^{16}O at an excitation energy of 5 MeV/nucleon.

The probability distribution reaches its peak at a multiplicity of 4 in the cases of Fermi breakup including only ground or particle-bound states (FB-GS and FB-PB) and falls fairly quickly at larger and smaller values of the multiplicity. In contrast, the two-fragment partition makes the dominant

contribution in the case in which the fragment excitation energies participate in the equilibrium, furnishing results very similar to that of an extended evaporation model.

4. Conclusion

Multifragmentation plays an important role in the statistical decay of light nuclei of biological interest. The statistical multifragmentation and extended Fermi breakup models take into account the large number of fragment states that can be excited in such decays, while the usual Fermi breakup model does not. Taking these states into account furnishes statistical properties, such as fragment temperatures and average kinetic energies, in better agreement with those of evaporation models of the decay. We are now studying the multiplicity dependence of the multifragmentation process in order to better calculate the secondary decay of the excited fragments.

References

[1] E. Fermi, *High energy nuclear events*, Progress of Theoretical Physics, v. 5, p. 570-583, 1950.

[2] J.P. Bondorf, R. Donangelo, I.N. Mishustin, C.J. Pethick, H. Schulz, K. Sneppen, *Statistical multifragmentation of nuclei (I)*, Nuclear Physics A, v. 443, p. 321-347, 1985.

[3] J.P. Bondorf, R. Donangelo, I.N. Mishustin, H. Schulz, *Statistical multifragmentation of nuclei (II)*, Nuclear Physics A, v. 444, p. 460-476, 1985.

[4] H.W. Barz, J.P. Bondorf, R. Donangelo, I.N. Mishustin, H. Schulz, *Statistical multifragmentation of nuclei (III)*, Nuclear Physics A, v. 448, p. 753-763, 1986.

[5] J.P. Bondorf, A.S. Botvina, A.S. Iljinov, I.N. Mishustin, K. Sneppen, *Statistical multifragmentation of nuclei*, Physical Reports, v. 257, p. 133-221, 1995.

[6] B.V. Carlson, R. Donangelo, S.R. Souza, W.G. Lynch, A.W. Steiner, M.B. Tsang, *Fermi breakup and the statistical multifragmentation model*, submitted for publication.

[7] R. Donangelo, K. Sneppen, S.R. Souza, *A computer program for statistical multifragmentation of nuclei*, Computer Physics Communications, v. 140, p. 405-411, 2001.

[8] R. Capote, M. Herman, P. Obložinský, P.G. Young, S. Goriely, T. Belgya, A.V. Ignatyuk, A.J. Koning, S. Hilaire, V.A. Plujko, M. Avrigeanu, O. Bersillon, M.B. Chadwick, T. Fukahori, Zhigang Ge, Yinlu Han, S. Kailas, J. Kopecky, V.M. Maslov, G. Reffo, M. Sin, E.Sh. Soukhovitskii and P. Talou, NDS **1**10 (2009) 3107; Available online at http://www-nds.iaea.org/RIPL-3/.